Nuclear Engineering and Technology 48 (2016) 285–292

Available online at ScienceDirect

Nuclear Engineering and Technology

journal homepage: www.elsevier.com/locate/net

Invited Article

Detection of Antineutrinos for Reactor Monitoring

Yeongduk Kim [a,b,*]

[a] Center for Underground Physics, Institute of Basic Science, Daejeon 34057, South Korea
[b] Department of Physics and Astronomy, Sejong University, Seoul 05006, South Korea

ARTICLE INFO

Article history:
Received 10 February 2016
Accepted 11 February 2016
Available online 18 February 2016

Keywords:
Gadolinium
Liquid Scintillator
Monitoring
Neutrinos
Oscillation
Reactor

ABSTRACT

Reactor neutrinos have been detected in the past 50 years by various detectors for different purposes. Beginning in the 1980s, neutrino physicists have tried to use neutrinos to monitor reactors and develop an optimized detector for nuclear safeguards. Recently, motivated by neutrino oscillation physics, the technology and scale of reactor neutrino detection have progressed considerably. In this review, I will give an overview of the detection technology for reactor neutrinos, and describe the issues related to further improvements in optimized detectors for reactor monitoring.

1. Neutrinos from nuclear reactors

Nuclear reactors are the most intense sources of antineutrinos, and it was natural that neutrinos were discovered in a detector located near a nuclear reactor [1]. Fission reactors produce fission fragments in highly excited states, and the neutron-rich fragments further decay, mainly by beta decays, emitting approximately six neutrinos per fission on average. As the energy released for each fission is ~200 MeV, we expect about 2×10^{20} neutrinos/s to be emitted from a 1-GW thermal power reactor. Neutrinos from beta decays are antineutrinos with negative helicity in contrast to the neutrinos from fusion reaction, which have positive helicity. We will simply refer to reactor antineutrinos as reactor neutrinos in this paper.

It was suggested that neutrinos from nuclear reactors may oscillate to other types (muon or tau) of neutrinos (neutrino oscillation), and many experiments were conducted near nuclear reactors until the year 2000. The detectors became bigger and the baseline became longer. In 2003, the KamLAND experiment, located at the Kamioka mine in Japan, finally detected the neutrino oscillation phenomenon for reactor neutrinos. The overview of these experiments is described in Section 4.

There are basically two methods to calculate the energy spectra of reactor neutrinos. The first uses an experimentally determined electron spectrum and converts it into a neutrino spectrum. The second method is to calculate all the beta decay branches using the allowed Coulomb correction in the spectral shape. The energy spectra for reactor neutrinos were

* *Corresponding author.*
E-mail address: ydkim@ibs.re.kr.
http://dx.doi.org/10.1016/j.net.2016.02.001

studied by King and Perkins [2] to understand the Reines data for the first time. The theoretical models to calculate the flux and energy spectra of reactor neutrinos were continually developed by Davis et al. [3], Vogel and Engel [4], Huber and Schwetz [5], Mueller et al. [6], and Huber [7], by combining the theories and experimental measurements from the beta decay of irradiated foils of four isotopes. The most recent model is the Huber + Mueller model, which gave parameterization for the energy spectra in a sixth-order polynomial form for each isotope.

$$\phi_\nu(E_\nu) = \exp\left(\sum_i^6 \alpha_i E_\nu^{i-1}\right) \quad (1)$$

Huber [7] has given the parameters for ^{235}U, ^{239}Pu, and ^{241}Pu isotopes, and Mueller [6] has determined the parameters for ^{238}U. Fig. 1 shows a comparison of the neutrino flux of the four isotopes normalized per fission drawn with the Huber + Mueller model.

The reactor neutrinos were detected through the capture process by the protons, which produces a positron and a neutron. The cross section of this process has been extensively studied by Vogel and Beacom [8], and the uncertainty of the cross section is known to be below 1%.

Fig. 2 shows the number of neutrino absorption events with the proton target as a function of neutrino energy. The calculation is done for a 1-GW reactor for each isotope with the initial isotopic configuration for 4% enriched fuel. The ^{235}U isotope contributes most to the neutrino events. The y axis shows a value for the total neutrino flux from the 1-GW reactor multiplied by the total cross section at the energy.

2. Detection of reactor neutrinos

Reactor neutrinos were first detected through the reaction of $\bar{\nu} + p \rightarrow e^+ + n$ [1]. This reaction is called the inverse beta decay (IBD) process, because it is the reverse process of neutron beta decay. For a few megaelectron volt neutrinos, the kinetic energy of the produced neutrons is a few tens of kiloelectron

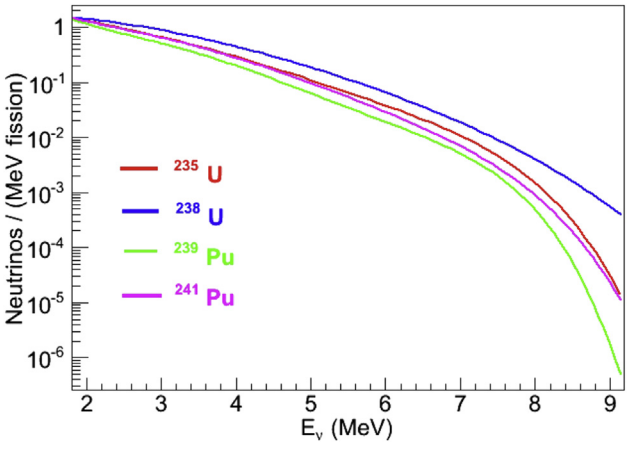

Fig. 1 – Number of neutrinos for each isotope in the nuclear reactor. The graphs are produced from the parameterization by Huber and Mueller.

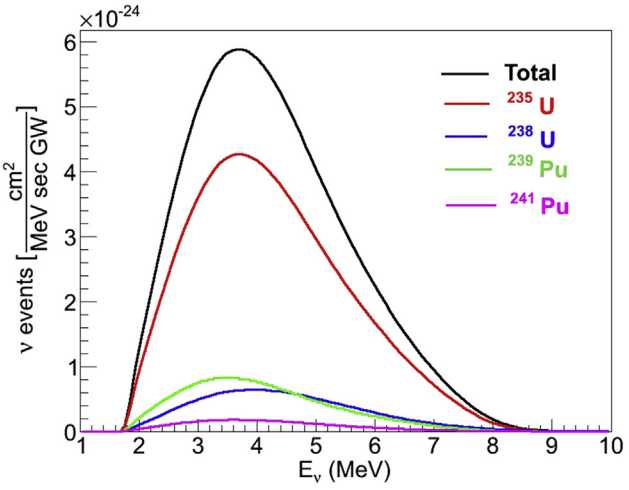

Fig. 2 – Number of events of the inverse beta decay of reactor neutrinos for each isotope. The y axis shows the total neutrino flux from a 1-GW reactor multiplied by the total cross section at the energy. The calculation is done with the initial isotopic configuration for 4% enriched fuel.

volts, so the neutrons are thermalized readily inside the liquid scintillator. Usually, liquid scintillator material contains hydrogen and carbon atoms in a ratio between 1:1 and 2:1. The threshold energy of the IBD process is 1.8 MeV; therefore, neutrinos below this energy have never been measured in the IBD process. In principle, other nuclear targets with lower threshold energies exist, but the low energy IBD process for other nuclear isotopes cannot produce neutrons with the low threshold. Without neutrons, it is difficult to reduce the background events; thus, nuclear targets other than the proton have not yet been used for reactor neutrino detection.

The kinetic energy of positrons corresponds to the initial neutrino energy, so that we can measure the neutrino energy by measuring the energy deposition by the positron. A positron annihilates with an electron in the liquid scintillator, giving out two 511-keV gamma rays. Therefore, the prompt energy, deposited by the positron including the annihilation energy, is related to the neutrino energy as:

$$E_{\text{prompt}} = E_\nu - 0.784 \text{ MeV}. \quad (2)$$

Fig. 3 shows a schematic layout of neutrino detection inside a typical detector. The combination of the positron and the neutron signals separated by an order of microseconds is a well-characterized event, which can be identified among a lot of background events such as high-energy gammas and fast neutrons.

The detection methods of reactor neutrinos depend on how to detect the neutrons produced by the IBD process. Table 1 shows the properties of the isotopes used for the detection of the neutrons. The elapsed time for the moderated thermal neutron to be captured by protons inside the liquid scintillator is ~180 μs. The process, $n + p \rightarrow d + \gamma$, has a Q value of 2.225 MeV, and emits a 2.2-MeV gamma ray, which is separated from the prompt positron signal. We can shorten the capture time by adding gadolinium by about 0.1% by weight into the central liquid scintillator [gadolinium-loaded liquid scintillator (Gd-LS)], called the "target"; then the

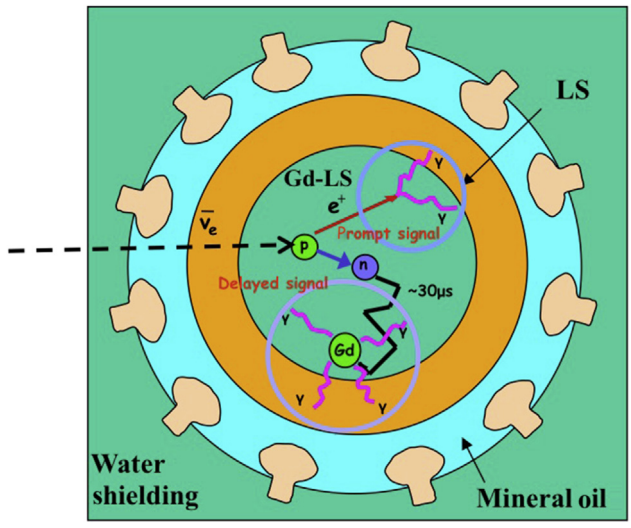

Fig. 3 – Schematic layout of antineutrino detector concept. Gd-LS is the liquid scintillator doped with natural Gd (target) and LS is liquid scintillator without Gd dopant (gamma catcher). Mineral oil is nonscintillating light transmitting material. LS should be ~60 cm to measure the gammas produced inside Gd-LS sufficiently. The Target scintillator can be doped with ^{6}Li instead of Gd, then the neutron capture signal is localized within a few mm range without gammas (see text). GD-LS, gadolinium-loaded liquid scintillator.

capture time is reduced to 30 μs. The capture process, $n + {}^{155(157)}\mathrm{Gd} \rightarrow {}^{156(158)}\mathrm{Gd} + \gamma$, emits several gammas with a total energy of ~8 MeV. One important point is that the positron signal (prompt signal) generates two 511-keV gammas from the annihilation of the positron inside the liquid scintillator. To prevent the leakage of 511-keV gammas from the target liquid scintillator, the target volume is surrounded by another layer of liquid scintillator of a few tens of centimeters thickness without gadolinium (LS). This liquid scintillator is called "gamma catcher," and the two liquid scintillators are viewed via common photomultiplier tubes (PMTs), which are usually immersed in nonscintillating mineral oil. The gamma catcher also detects the gammas from neutron capture on gadolinium isotopes; therefore, the neutron capture signal can be close to the total energy release of 8 MeV. To fully collect the gammas for the events occurring at the boundary of the target liquid scintillator, the thickness of the gamma catcher should be larger than 60 cm.

One can load ^{6}Li instead of gadolinium for neutron capture in the target liquid scintillator, in which case a process of $n + {}^6\mathrm{Li} \rightarrow \mathrm{t} + {}^4\mathrm{He}$ captures the thermal neutrons with a Q value of 4.783 MeV. In this case, the released energy is in the form of kinetic energy of the triton and alpha particles, and the pulse shape discrimination property of the liquid scintillator can separate the neutron capture signal from the abundant gamma backgrounds. Although it releases 4.783 MeV, the signal is about 0.6 MeV owing to the quenching effect of the low energy ions in the liquid scintillator. In the case of ^{10}B, the Q value is only 2.790 MeV, and it emits 0.48 MeV gammas most of the time [9]. Therefore, in general, ^{6}Li doping is better to use for neutrino detection than Boron doping. However, ^{6}Li should be enriched for use because of the low natural abundance of ^{6}Li.

3. Review of previous experiments

Before the Kamiokande experiment confirmed the neutrino oscillation phenomenon [10], many experiments were conducted to detect this phenomenon by measuring the reactor neutrinos at different baselines. First, the detectors were located a few tens of meters from the reactors and compared with the theoretical expectations. One of the largest detectors was built for the Chooz experiment, which had a 5-ton liquid scintillator with 0.1% Gd-LS. In 2002, the Japanese liquid scintillator detector that had about 1 kton of liquid scintillator was built at Kamioka mine. Surprisingly, this KamLAND experiment found that the reactor neutrinos do indeed maximally oscillate at the baseline of 50 km. The KamLAND detector did not use gadolinium dopant because hydrogen capture was sufficient to measure the neutrons from the IBD process with the very low background rate owing to the deep (1,000 m) underground location of the detector. Table 2 lists certain experiments that measured reactor neutrinos for the past 3 decades, including the detector, the shielding structure, and the neutrino rates measured. It does not include all the experiments, but most experiments that gave sufficient details of the data are included.

Table 1 – The properties of isotopes to be used to capture neutrons from the IBD process.

Isotope	Abundance (%)	Cross section (barn)	Capture time (μs)[a]	Q value (MeV)[b]
^{1}H	99.985	0.294	180	2.225
^{155}Gd	14.8	60,740	30 (0.1 W%) for natural Gd	8.535
^{157}Gd	15.65	253,700		7.936
^{6}Li	7.6	940	30 (0.15 W%) for 90% enriched ^{6}Li	4.783
^{7}Li	92.4	0.045		–
^{10}B	19.9	3,835	1.4 (5% W%) for natural B	2.790 (6%) 2.312 + 0.478 MeV γ (94%)
^{11}B	80.1	0.005		–

IBD, inverse beta decay.
[a] The capture time is given for natural gadolinium, natural boron, and enriched ^{6}Li in liquid scintillator with the specified concentration by weight.
[b] The Q values are from [9].

Table 2 – A summary table for the experiments conducted until 2015 to measure reactor neutrinos.

Exp	P (GW)	Fuel ^{235}U %	Detector	Shielding	Mass (ton or L)	Depth MWE	L m	Time (d) on–off	ε %	No. of events #/day On–Off	S/B	Ref.
Bugey3	2.8		^{6}Li(0.15%) + LS (NE320) Seg. 98	8 cm LS 4 mm B_4C 25 cm water 10 cm Pb	0.556 (600 L)	23 9.5	15 40 95	72–60 129–72 28–6	~20	1,285–62 251–66 67–37	21 3.8 1.8	[11]
Bugey4	2.8		^{3}He + H_2O	10 cm LS 4 mm B_4C 25 cm water 10 cm Pb	1.48	25	15	88–39	54.9	5,621–2,599	1.16	[12]
Goesgen	2.8		^{3}He + LS(NE235C) SEG. 30	5 mm B_4C 20 cm water 15 cm iron 2 m concrete	377 L	5	38 46 65	143 204 359	16.7 16.5 16.8	76– 52– 24–	~4 ~3 ~1.5	[13]
ILL	0.057	93	^{3}He + LS(NE235C) SEG. 30	12 cm LS 15 cm PE 20 cm Pb	0.325 (377 L)	8	8.76	129–49	19.4	38–	1~2	[14]
Palo Verde	11.63		Gd-LS (0.1%) (seg.,66)	1 m H_2O	11.34	32	750 890	350–	11.2	~50–	~1	[15]
Chooz	8.5	3.1	Gd-LS	1–2 m LS 75 cm SAND 14 cm FE	5	300	1,000	64–143	69.8	25–1.4	18	[16]
SRP	2.0	–	Gd-LS (0.5%) NE313	~10 inches LS veto 2 inches Pb 3 inches plastic veto 8 inches Pb	275 L	–	18.2 23.8	172– 208–	37.7	419– 260–	–	[17]
SONGS	3.4		Gd-LS (0.1%) Seg. 4	0.5 m H_2O	0.64	25	25	–	~10	564–105	5.5	[18]
KamLAND		–	Spherical LS (diam. 13 m)	180 cm oil veto ~1 m water	1,000	2,700	~180,000	~1,930–	~90	0.83–0.14	5.8	[19]
Double Chooz	8.5	4	Gd-LS	55 cm LS 105 cm oil 50 cm LS 15 m steel	8	300	1,050	461–	91.5	37.7–1.6	23.6	[20]
Daya Bay	17.4	4	Gd-LS	45 cm LS 50 cm oil 2.5 m water	20	250 265 860	360 500 1,580	565– 568– 562–	80 83.7 96.3	664–13 595–9.5 74–2.2	51 63 34	[21]
RENO	16.8	4	Gd-LS	60 cm LS 70 cm oil 150 cm water	16	120 450	290 1,380	500– 500–	64.7 74.5	617–17.5 61.2–3.1	35 19.7	[22]
NEOS	3.0	4	Gd-LS	10 cm Bo-PE 10 cm Pb	1	30	23.6	30	~50	1,946–84	22	[23]

Gd-LS, gadolinium-loaded liquid scintillator; ILL, Institut Laue-Langevin; NEOS, Neutrino Experiment for Oscillation at Short baseline; S/B, signal/background; SONGS, San Onofre Nuclear Generating Station; SRP, Savannah River Plant.

In the United States, an experiment at San Onofre Nuclear Generating Station (SONGS; Pendleton, CA, USA) tried to detect the reactor neutrinos to monitor the reactor thermal power and possibly the fuel composition. As shown in Fig. 2, the neutrino spectra from the four different isotopes are slightly different; therefore, in principle it is possible to measure the fractions of the isotopes by precisely measuring the energy spectra from the reactors. The SONGS experiment measured the total number of neutrinos as a function of elapsed time after the replacement of the fuels. The data and predicted rates of the SONGS detector are shown in Fig. 4. It observed a reduction of ~10% in the neutrino event rates in a period of about 500 days, even though the thermal power from the reactor was constant for that period [24,25]. As the detector was not optimized for precise energy measurement, the energy spectrum was not studied extensively in the SONGS experiment. With the rate only, the amount of ^{239}Pu being produced or removed from a reactor could be constrained to the 100-kg level [25]. If the new detectors at short baseline can precisely measure the energy spectrum, the sensitive amount of ^{239}Pu will be reduced.

In 2008, a workshop was held by the International Atomic Energy Agency on antineutrino detection for safeguards applications. The workshop concluded that the antineutrino detectors have unique abilities to nonintrusively monitor reactor operational status, power, and fissile content in real time, from outside containment [24]. It also recommended the International Atomic Energy Agency to consider antineutrino detection and monitoring in its current R&D program for safeguarding bulk-process reactors [24]. The optimized

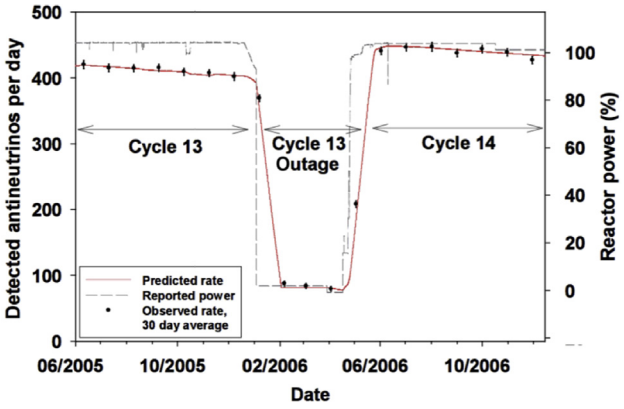

Fig. 4 – Monthly neutrino rates observed by the SONGS detector. It shows the evolution due to changes in the fissile content from burnup. Taken from Fig. 2 in Ref. [24]. It shows the possibility to monitor the reactor fuel contents by measuring the neutrino rates. SONGS, San Onofre Nuclear Generating Station.

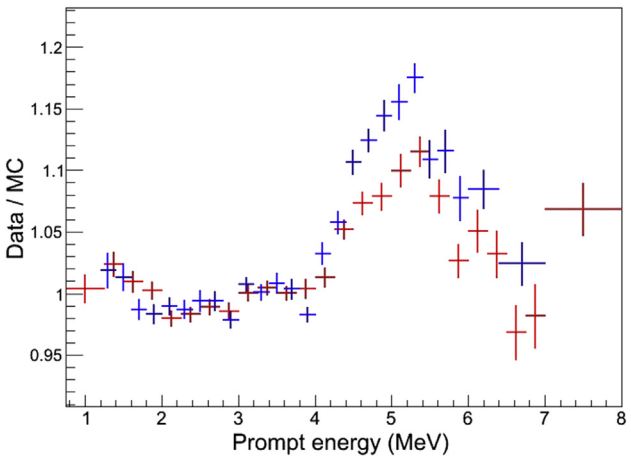

Fig. 5 – Data of the RENO (blue) and Daya Bay (red) experiments divided by the Monte Carlo calculations with Huber + Mueller model. Both experiments showed the unexpected bump between 4 MeV and 6 MeV energy region, although the RENO saw a larger excess than the Daya Bay experiment [21,22].

neutrino detector for reactor monitoring and safeguards should be relatively compact in size and preferably movable. Many proposals to achieve the goal have been made, and prototype detectors have been tested as described in Section 4.

After the KamLAND detector successfully observed the reactor neutrino oscillation, three large detectors were built to measure another neutrino oscillation at kilometer-scale baseline: Double Chooz (Chooz, France), Daya Bay (Daya Bay, China), and RENO (Yongkwang, Korea) detectors. These experiments were very successful in measuring the new neutrino oscillation parameter. In addition, these experiments could measure the neutrino energy spectrum more precisely because they had sufficiently thick gamma catchers and very low background levels. The energy resolutions of these experiments were 7–8% in standard deviation at 1 MeV, and compared well with the Huber + Mueller model. Unexpectedly, these experiments observed deviations from the predicted spectra at ~5 MeV energy in the prompt energy spectra. There were more neutrinos at this energy region than expected rates, and the excesses were between 1% and 3% of the total neutrinos. Fig. 5 shows the ratio of the measured prompt energy spectra divided by the expected spectra by the Huber + Mueller model as shown in Fig. 2. Actually, the Chooz experiment already observed this excess in 2003 [16], but it was not noticed at that time. At present, it is not yet well understood what causes the excess at the 5-MeV energy region. Hayes et al. [26] proposed three possibilities for the excess: (1) ^{238}U uncertainty is large and this isotope may contribute to the excess; (2) epithermal neutron contribution to the fission rate in the reactor core contributes to the excess; and (3) Institut Laue-Langevin (ILL)'s beta measurement has an error.

4. Toward more precise energy spectra for reactor neutrinos

Because the energy resolution of the liquid scintillator is limited by the photoelectron statistics for most of the detectors constructed up to the present, we can improve the energy resolution by increasing the coverage of the PMT photocathodes. Indeed, the recently proposed Jiangmen Underground Neutrino Observatory (JUNO) experiment aims to measure the reactor neutrinos with an energy resolution of ~3% in standard deviation by increasing the number of PMTs to 18,000 [27]. However, the energy spectra of the JUNO detector will be dominantly distorted by the neutrino oscillations.

To measure the neutrino energy spectrum more precisely, a small detector located within a few tens of meters can obtain the spectra with similar energy resolution. The photoelectron statistics can be improved to >1,000 photoelectrons/MeV, and we can make the energy resolution about 3–4%. The gamma catcher can be also adopted in the design. The attenuation length of 511-keV gammas is about 10 cm in the liquid scintillator, and the neutron capture length in liquid scintillator is about 9 cm on average. Therefore, the IBD events occurring at the gamma catcher can be misidentified as IBD events occurring at the target scintillator if the neutrons are captured by the gadolinium isotopes in the target Gd-LS. We call these events "spill-in." If the gamma catcher is not thick enough, these spill-in events will have some leakage of the two 511-keV gammas, and deteriorate the energy resolution of the whole IBD events. Therefore, the thickness of the gamma catcher should be much larger than the attenuation length of 511-keV gammas.

In Fig. 3, the thickness of the gamma catcher could be 40 cm, and the diameter of the target liquid scintillator can be 100 cm (450 kg). The mineral oil layer is 40 cm thick, and the PMTs are immersed in the mineral oil. For shielding, 10 cm lead will surround the liquids. Then, the total size would be ~300 cm. To avoid spill-in contribution, it would help to use the boron-loaded liquid scintillator (5% natural boron) in the gamma catcher layer and mineral oil layer. Then the neutrons from the IBD events occurring in the outer part of the gamma

catcher will be mostly absorbed in ^{10}B and cannot satisfy the requirements for the delayed neutron capture signal. Therefore, the spill-in events will not lose the 511-keV gammas and the energy resolution will be improved. The two 511-keV gammas of the IBD events occurring at the target will be detected, and the energy reconstruction of the prompt energy will be close to perfect with the 40-cm-thick gamma catcher. Here, one should be careful to make the scintillation efficiency of Gd-LS (target) and boron-loaded LS (gamma catcher) the same for good energy resolution.

In this optimized reactor neutrino detector, PMTs will cover almost all of the surface area, and the coverage would be ~75% with 80 8-inch PMTs for the above configuration. Then, we can expect ~1,500 photoelectrons/MeV with which we can achieve ~2.5% energy resolution for the 1-MeV signal. For the 5-MeV energy region, we expect better than 1.5% energy resolution and this will substantially improve our current understanding of the neutrino spectrum from reactors.

There are many proposals for the monitoring of nuclear reactors with segmented detectors. The PROSPECT detector is an array of 10 × 12 configuration, 120 segments [28], and the PANDA [29] is also a segmented detector. Each segment is 120 cm long with 14.5 cm × 14.5 cm cross section in a bar shape and optically decoupled from adjacent bars, and the segment is ^{6}Li-loaded plastic scintillator that will have about 4.5% energy resolution for 1 MeV prompt energy. This design has a disadvantage in that the range of MeV positrons are approximately in centimeters, so it is not negligible because the positrons hit the wall material and lose the energy information. In this respect, the homogeneous detector is superior to the segmented detectors. The segmented detector design has the advantage of reducing the background by hit pattern identification.

One promising design is the NuLat (short for neutrino lattice) detector [30]. It is composed of a 15 × 15 × 15 cubic array of 3,375 individual cubes of ^{6}Li-doped plastic scintillator, 6.4 cm on a side. These cubes are stacked and separated by about 0.3 mm air gap between them, and there is no wrapping material for the cubes. The scintillation lights are propagated by the internal total reflection through the cubes along the three axes, and also scattered in an off-axis direction. In this way, the event is localized in a cube without any energy loss in wrapping materials. Two 511-keV gammas of the prompt signal will be measured by the neighboring cubes. All six surfaces of the array will be viewed by a 2-inch PMT, and then the total number of PMTs is 1,350. The NuLat detector is ideal because there is no energy loss, there is no light loss in principle, and it has sufficient segmentation to reduce the backgrounds. The plastic scintillator also has a good Pulse Shape Discriminations (PSD) capability to further reduce the backgrounds from fast neutrons. The group should demonstrate that the energy resolution is better than 5% at 1 MeV energy with a sufficiently big array, which requires fine machining. Although this configuration is optimized to reduce the backgrounds, the energy resolution will be worse than the configuration we described for the homogeneous multilayer Gd-LS target detector.

Another short baseline detector, NEOS (Neutrino Experiment for Oscillation at Short baseline), was built to yield a reliable measurement of the reactor neutrino anomaly [31]. The group developed 0.5% Gd-loaded LS, based on the mixed solvents of Linear alkylbenzene (LAB) and Ultima Gold F liquid scintillator produced by PerkinElmer (PerkinElmer Biotechnology Company, Waltham, MA, USA) in a 9:1 ratio. This mixture shows a good PSD power with high light output. Quality controls were applied at each stage of the mixing procedure, such as checks on the light yield, Gd concentration, transmittance, density, and water content. It contained ~1,000 L Gd-LS, in a cylindrical shape, viewed by the two end caps with 38 eight-inch PMTs. The target scintillator was shielded with borated polyethylene plates of 10 cm thickness, lead of 10 cm thickness, and plastic scintillators of 5 cm thickness for muon veto. The NEOS experiment started to take data starting in August 2015 inside the tendon gallery of the fifth nuclear reactor of Hanbit nuclear power plant in Korea [23]. As shown in Table 2, the NEOS detector obtained a signal/background ratio of >20 mainly because of the large overburden of the tendon gallery, ~30 m water equivalent depth. NEOS will suffer from the leaking of 511-keV gammas, although it has ~5% resolution at 1 MeV prompt energy.

Another important aspect is the energy calibration. As there is no monoenergetic electron source, the detectors are usually calibrated by a radioactive gamma source. However, gamma rays generate multiple electrons because of the Compton scattering of the gamma rays inside the liquid scintillator. Then the light output from the position may be different from the electrons from the gamma source. This is mainly due to the Cherenkov photons produced by the energetic electrons or positrons. We can calculate the number of Cherenkov photons as a function of the wavelength, but we do not understand sufficiently well the conversion of the Cherenkov radiation into visible light from the scintillator. The UV Cherenkov photons should be absorbed in LAB-based liquid scintillator, and then be reemitted as larger-wavelength photons. The efficiency of the conversion as a function of photon wavelength is neither known well nor measured yet.

It is possible to measure the Cherenkov photon efficiency with high-energy gammas and HPGe detector for the Compton scattered gammas, which will generate electrons with calculable energy inside the Gd-LS. It has been demonstrated that a 6-MeV proton beam on a thick natural carbon target is an efficient way to generate 4.44-MeV gammas [32,33]. The resonant reaction of 5.3 MeV protons with ^{12}C to $^{13}N^{*}$, and subsequent beta decay of ^{13}N to $^{12}C^{*}$(4.44MeV) produces a few mCi activity of 4.44 MeV gammas at the carbon target with a few microampere proton beam at a tandem facility. If we position a liquid scintillator cell attached to a PMT at 50 cm from the carbon target, the 4.44-MeV gamma flux will be 3,500 $\gamma/cm^2/s$.

5. Discussion

Reactor neutrino detection technology is developing rapidly because there are motivations for neutrino oscillation studies at medium and short baselines. The detectors will be ton-scale for short baseline experiments and 20-kton scale for medium baseline. In another respect, neutrinos at short baseline are useful for the monitoring and safeguards technology for nuclear

reactors. The detector technology is common in many aspects for the two purposes. For both projects, the background reduction is very difficult to achieve, and the background simulation could not yet satisfactorily reproduce the background rates.

Because the optimized detector is relatively large (~3 m in 3 dimensions), the current tendon gallery (3 m in width and 4 m in height) is not sufficiently wide. Also, it should be advantageous to be closer to the reactor because the target mass of the proposed detector configuration is 500 kg. Therefore, I would like to propose an extension of the tendon gallery toward the direction of the reactor with an additional tunnel of 10 m length. It could be 6 m in width and 4 m in height, as shown in Fig. 6. Then, the optimal detector can be easily housed, the distance of the detector to the reactor can be varied, and the dependence of the energy spectra on the burnup can be accurately measured. This modified tendon gallery can be realized in one of the new commercial reactors planned in Korea, such as Shin Hanul #3 or #4 reactor. The data anticipated in this configuration can surpass the quality of all other reactor experiments, and we can study the feasibility of the reactor monitoring power with the reactor neutrinos better.

To achieve energy resolution better than 3% for reactor monitoring and a better understanding of the neutrino energy spectra, one needs careful design of the detectors and their optical properties. A three-dimensional segmentation design or multilayer homogeneous design are promising configurations for the detector at shallow overburden, and the community will continue to test new ideas to overcome the backgrounds and enhance energy measurements for reactor neutrinos.

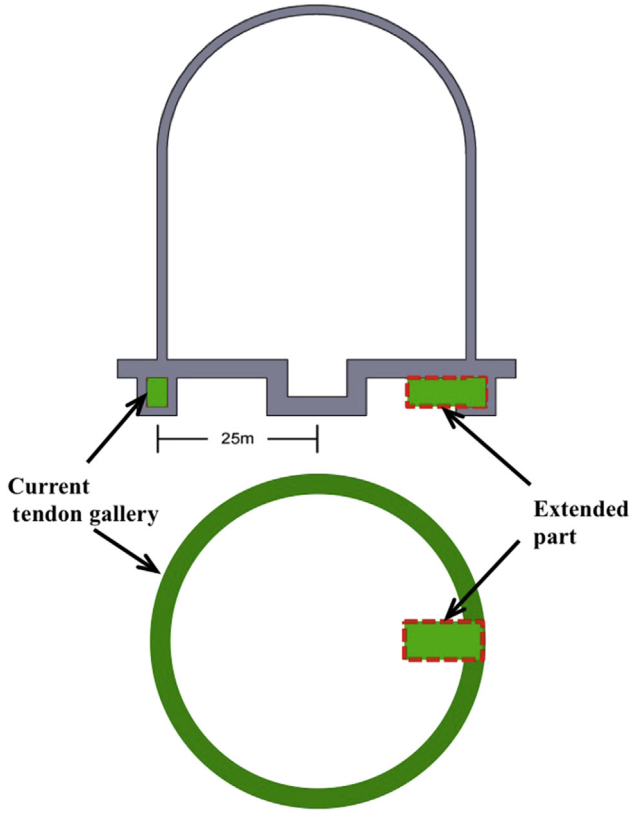

Fig. 6 – Schematic view of the current tendon gallery and a proposed extension of the tendon gallery toward to the reactor core. This can be incorporated in the design of the newly constructed commercial reactor.

Conflicts of interest

The author declares no conflicts of interest.

Acknowledgments

This work was funded by Grant Nos IBS-R016-D1 and 2012M2B2A6029111 from National Research Foundation (NRF). The author appreciates the Korea Hydro and Nuclear Power (KHNP) company (1655, Bulguk-ro, Gyeongju-si, Gyeongsangbuk-do, Korea 38120) and the director of third nuclear plant of Hanbit nuclear power site for the permission to set up the neutrino detector at the tendon gallery of the reactor.

Nomenclature

GW	Gigawatt (10^9 W)
E	Energy
eV	Electron volt (1.6×10^{-19} J)
keV	Kiloelectron volt
MeV	Megaelectron volt
P	Power
L	Distance from reactor to detector
S/B	Signal/background ratio
PMT	Photomultiplier tube

Greek Letters

ν	Neutrino
ε	Efficiency
ϕ	Flux

REFERENCES

[1] C.L. Cowan, F. Reines, F.B. Harrison, H.W. Kruse, A.D. McGuire, Detection of the free neutrinos: a confirmation, Science 124 (1956) 103–104.
[2] R.W. King, J.F. Perkins, Inverse beta decay and the two-component neutrino, Phys. Rev. 112 (1958) 963–966.
[3] B.R. Davis, et al., Reactor antineutrino spectra and their application to antineutrino-induced reactions, Phys. Rev. C 19 (1979) 2259–2266.
[4] P. Vogel, J. Engel, Neutrino electromagnetic form factors, Phys. Rev. D 39 (1989) 3378–3383.
[5] P. Huber, T. Schwetz, Precision spectroscopy with reactor antineutrinos, Phys. Rev. D 70 (2004) 053011.
[6] Th.A. Mueller, et al., Improved predictions of reactor antineutrino spectra, Phys. Rev. C 83 (2011) 054615.
[7] P. Huber, Determination of antineutrino spectra from nuclear reactors, Phys. Rev. C 84 (2011) 024617. Erratum, Phys. Rev. C85 (2012) 029901.
[8] P. Vogel, J.F. Beacom, Angular distribution of neutron inverse beta decay, $\bar{\nu} + p \rightarrow e^+ + n$, Phys. Rev. D 60 (1999) 053003.
[9] www.nndc.bnl.gov.

[10] Y. Fukuda, et al., Evidence for oscillation of atmospheric neutrinos, Phys. Rev. Lett. 81 (1998) 1562–1567.
[11] M. Abbes, et al., The Bugey 3 neutrino detector, Nucl. Instrum. Methods A 374 (1996) 164–187.
[12] Y. Declais, et al., Study of reactor antineutrino interaction with proton at BUGEY nuclear power plant, Phys. Lett. B 338 (1994) 383–389.
[13] G. Zacek, et al., Neutrino-oscillation experiments at the Gosgen nuclear power reactor, Phys. Rev. D 34 (1986) 2621–2636.
[14] H. Kwon, et al., Search for neutrino oscillations at a fission reactor, Phys. Rev. D 24 (1981) 1097–1111.
[15] A. Piepke, Final results from the Palo Verde neutrino oscillation experiment, Phys. Rev. D 64 (2001) 112001.
[16] M. Apollonio, et al., Search for neutrino oscillations on a long base-line at the Chooz nuclear power station, Eur. Phys. J. C 27 (2003) 331–374.
[17] Z.D. Greenwood, et al., Results of a two-position reactor neutrino-oscillation experiment, Phys. Rev. D 53 (1996) 6054–6064.
[18] N.S. Bowden, et al., Observation of the isotopic evolution of pressurized water reactor fuel using an antineutrino detector, J. Appl. Phys. 105 (2009) 064902.
[19] S. Abe, et al., Precision measurement of neutrino oscillation parameters with KamLAND, Phys. Rev. Lett. 100 (2008) 221803.
[20] Y. Abe, et al., Improved measurements of the neutrino mixing angle θ_{13} with the double Chooz detector, J. High Energy Phys. 10 (2014) 086.
[21] F.P. An, et al., New measurement of antineutrino oscillation with the full detector configuration at Daya Bay, Phys. Rev. Lett. 115 (2015) 111802.
[22] J.H. Choi, et al., Observation of Energy and Baseline Dependent Reactor Antineutrino Disappearance in the RENO Experiment, arXiv:1511.05849, 2015.
[23] Y. Oh, Neutrino Experiment for Oscillation at Short Baseline, Presentation at Applied Antineutrino Physics 2015 Workshop, Virginia Tech Research Center in Arlington, VA.
[24] Final Report: Focused Workshop on Antineutrino Detection for Safeguards Applications, 28–30 October 2008, IAEA Headquarters, Vienna, 2008.
[25] N.S. Bowden, et al., Experimental results from an antineutrino detector for cooperative monitoring of nuclear reactors, Nucl. Instrum. Methods A 572 (2007) 985–998.
[26] A.C. Hayes, et al., Possible origins and implications of the shoulder in reactor neutrino spectra, Phys. Rev. D 92 (2015) 033015.
[27] Djurcic, et al., JUNO Conceptual Design Report, arXiv:1508.07166, 2015.
[28] J. Ashenfelter, et al., The PROSPECT Physics Program, J. Instrum. 11 (2015) P11004.
[29] S. Oguri, et al., Reactor antineutrino monitoring with a plastic scintillator array at a new safeguards method, Nucl. Instrum. Methods. A 757 (2014) 33–39.
[30] C. Lane, et al., NuLat: A New Type of Neutrino Detector for Sterile Neutrino Search at Nuclear Reactors and Nuclear Nonproliferation Applications, arXiv:1501.06935, 2015.
[31] G. Mention, et al., Reactor antineutrino anomaly, Phys. Rev. D 83 (2011) 073006.
[32] H. Wan Chan Tseung, et al., Measurement of the dependence of the light yields of linear alkylbenzene-based and EJ-301 scintillators on electron energy, Nucl. Instrum. Methods A 654 (2011) 318–323.
[33] P. Dyer, et al., Cross sections relevant to gamma-ray astronomy: proton induced reactions, Phys. Rev. C 23 (1981) 1865–1882.